Structural Engineering and Mechanics, *Vol. 75, No. 3 (2020) 283-294*
DOI: https://doi.org/10.12989/sem.2020.75.3.283

Multi-Beams modelling for high-rise buildings subjected to static horizontal loads

Luca Sgambi*

Faculty of Architecture, Architectural Engineering and Urban Planning, Université catholique de Louvain, Louvain-la-Neuve, Belgium

(Received October 19, 2019, Revised January 10, 2020, Accepted January 11, 2020)

Abstract. In general, the study of a high-rise building's behaviour when subjected to a horizontal load (wind or earthquake) is carried out through numerical modelling with finite elements method. This paper proposes a new, original approach based on the use of a multi-beams model. By redistributing bending and axial stiffness of horizontal elements (beams and slabs) along vertical elements, it becomes possible to produce a system of differential equations able to represent the structural behaviour of the whole building. In this paper this approach is applied to the study of bending behaviour in a 37-storey building (Torre Pontina, Latina, Italy) with a regular reinforced concrete structure. The load considered is the wind, estimated in accordance with Italian national technical rules and regulations. To simplify the explanation of the approach, the wind load was considered uniform on the height of building with a value equal to the average value of the wind load distribution. The system of differential equations' is assessed numerically, using Matlab, and compared with the obtainable solution from a finite elements model along with the obtainable solutions via classical Euler-Bernoulli beam theory. The comparison carried out demonstrates, in the case study examined, an excellent approximation of structural behaviour.

Keywords: multi-beams system; high-rise building; structural modelling; structural mechanics

1. Introduction

Today, high-rise buildings are at the forefront of modern engineering, due to their functional and structural characteristics. The issue of structural analysis with regards to such buildings is the subject of many current studies, with the aim to better describe their structural behaviour and improve their design techniques (Lee *et al.* 2014, Wu *et al.* 2017, Qiao *et al.* 2017, Alavi and Rahgozar 2018).

A significant number of studies focus on the analysis and design of systems aimed at contrasting horizontal loads on high-rise building. In Seon Park *et al.* (2016) a structural outrigger system is analysed and optimised through genetic optimisation in an attempt to identify the best position for the outriggers on a prototype model. Asai and Watanabe (2017) propose an improved outrigger system, TIMET (tuned inertial mass electromagnetic transducer), capable of increasing dissipated energy and recovering it in terms of electricity. The structural response of these buildings is essentially assessed numerically, through a finite element method (Brunesi *et al.* 2016, Avini *et al.* 2019, Tien and Calautit 2019) or experimentally with regards to certain issues. For instance, Soudian and Berardi (2017) experiment on the thermal energy storage capabilities in a building in Toronto while Sofi *et al.* (2018) are developing an experimental method based on the use of an interferometric radar system in order to determine the dynamic characteristics of a high-rise building.

This study focuses on modelling a multi-storey high-rise building. Specifically, it proposes a formulation based on differential equations that are capable of reproducing, with significant accuracy, the results of the finite elements model a building. In this first study, only a planar model will be analysed.

Structural modelling is the civil engineering activity that deals with providing mathematical representations of structures so that it is possible to obtain information (displacements and internal actions) for dimensioning and verifying the structural behaviour of a building. A structural model is therefore a "representation" and, as such, is an approximate reproduction of reality (Bateson 1979, Sgambi *et al.* 2013, Sgambi, 2016). In the context of structural engineering, the main modelling methods derive from two distinct approaches: a differential approach (or strong form) (Timoshenko 1970, Malerba and Sgambi 2014, Aydin and Bozdogan 2016, Wang *et al.* 2016) and a variational approach (or weak form) (Wallerstein 2001, Bayat and Pakar 2015, Bayat and Pakar 2017, Niiranen and Niemi, 2017).

In the differential approach, the continuum is conceived as divided into infinitesimal elements of matter and, under specific kinematic and material hypotheses, theories capable of describing the behaviour of many structural elements are developed. These theories require the formulation and solution of one or more differential equations with their respective boundary conditions. Renowned and frequently used are the Euler-Bernoulli (Barretta *et al.* 2015) or the Timoshenko (Civalek and Kiracioglu 2010) beam formulations, the Kirchhoff–Love theory of plates, etc. (Falsone 2018, Manju and Mukherjee 2019). These formulations are very efficient in the study of the behaviour of individual elements (a beam or a plate) but

*Corresponding author, Assistant Professor
E-mail: luca.sgambi@uclouvain.be

http://www.techno-press.com/journals/sem&subpage=7

ISSN: 1225-4568 (Print), 1598-6217 (Online)

they lose their effectiveness when the structure to be analysed is composed of several elements (such as the case of a bridge or a building containing beams and pillars). Indeed, formulation via differential equations and their solution are only used for studying relatively simple structures (for example, the displacements of a beam under a distributed load or the horizontal displacement of a simple frame). More complex structures require the composition and solution of a significant number of boundary conditions; thus, the differential approach tends to not be used in studying the structural behaviour of a building.

The numerical formulation derived from the differential approach is the finite differences method (Cyrus and Fulton 1966) where the differential problem is transformed into an algebraic problem. Even this formulation today lacks use due to the wide-spread presence of the finite element method. It remains a valid method for the numerical solution to problems th*et al*so involve the temporal dimension (Carrino *et al.* 2019) and other specific modelling issues (Feras 2015).

The second approach requires the formulation of the elasticity problem in its variational form. This formulation, equivalent to the differential formulation, requires the use of energy-related concepts applied to finite volumes of a continuum. The variational formulation of the elasticity problem has gained a greater level of success since it is at the foundation of the finite element method, currently the most used method for studying the structural behaviour in civil engineering (Bathe 1995, Garavaglia *et al.* 2013, Petrini *et al.* 2020, Lazzari 2019, Bathe 2019). High-rise and other buildings are in fact analised by modelling the beams, pillars and other structural elements using finite elements that give a numerical response to the structural behaviour at certain points (nodes and gauss points) of the model. The global response of structures is reproduced through an interpolation of local responses.

The following sections will demonstrate how it is possible to formulate the bending problem of a high-rise building in a differential form, limiting the number of equations and boundary conditions. The formulation will be carried out considering a planar modelling of the problem and in relation to a real example, the Torre Pontina, a 37-storey building with a reinforced concrete structure. Assuming that it is possible to distribute the stiffness of the slabs on the vertical structures it will be possible to achieve a model made up of various Euler-Bernoulli beams interconnected by an infinite number of springs. This particular structural system will be called multi-beams (MB) system.

It is worth noting that over in recent years several researchers have begun to study these systems of interconnected beams, both in numerical and analytical form, although most studies refer to systems consisting of only two coupled beams. For instance, Oniszczuk (2000) investigates the free vibrations of two Euler-Bernoulli beams joined by an infinite series of springs (dual-beams system). Vu *et al.* (2000), again for a dual-beams system, present an exact method for assessing the vibration characteristics when the system undergoes harmonic excitation. Abu-Hilal (2006) investigates the dynamic behaviour of a couple of Euler-Bernoulli beams joined together by an infinite series of springs and dampers subjected to a dynamic load. Pavlović *et al.* (2012) investigate the dynamic instability, of a dual-beams system, in the presence of random forces. In Han *et al.* (2018) and in Liu and Yang (2019) solutions in a closed form are researched for vibration analysis of elastically connected double-beam systems.

A high-rise building is a complex structure. The study and design of these structures require different analytical and numerical modelling according to the problems that have to be investigated. In fact, many particular mechanical-structural aspects intervene in the definition of the global and local response of this type of structure. These include, for example: the deformability of the foundation, which often has to be investigated considering the shear deformability of the plates (Civalek and Acar 2007), the interaction between the foundation and the ground (Akgoz and Civalek 2011), the identification of the stiffness of the connections (Lou and Wang 2015), the correct definition of the bending and shear deformability of the vertical resistant mechanisms (frames and shear walls) and the shear deformability of deep beams and floors (shear lag).

In this context, the use of simplified proxy models is crucial, especially for Monte Carlo (Sgambi *et al.* 2014) or optimisation analyses (Franchin *et al.* 2018) in the modern context of performance-based design under different hazards (Barbato *et al.* 2020).

Cuni *et al*. (2013) develop two simplified models (the first based on Timoshnko's theory and the second based on Eulero Bernoulli's theory) in which each floor of the structure is schematised by a node. To identify the flexural stiffness and shear of the models, the authors propose a calibration criterion to identify the value of some parameters (Young's modulus, shear modulus, density mass). The resulting values of these parameters, on which the flexural behaviour of the structure depends, lose all physical meaning (Cuni *et al*. 2013).

A further simplified model capable of considering flexural and shear deformability of the structure is developed by Fujita *et al*. (2015). Like the previous model, also the Fujita's model is an ideal model and requires an identification process to make the ideal model equivalent to the real behaviour of the structure. This identification process must be performed for each load scenario considered (Fujita *et al*. 2015).

The MB approach proposed in this paper is less effective (it requires more computational time to obtain a solution) than the approaches proposed by Cuni and Fujita. However, the MB approach provides an analytical description of the behaviour of the whole structure without any calibration procedure.

2. The case study

The approach proposed in the present paper is used to model the behaviour under horizontal load of a real structure. As a case study, Torre Pontina, a residential and office building located in the Municipality of Latina (Italy), was chosen. The aim of this paper is to present a model able to describe the static bending behaviour of the building based on differential equations. It must be noted that the purposes of this study do not include the precise evaluation of the structural response of the tower, therefore a number of simplifications will be made with regards to the structure in order to best focus the attention on the proposed formulation and its comparison with some benchmarks of reference.

Fig. 1 The Torre Pontina during construction (photo credit: Shapiro1983, Public Domain image)

Reaching 128 m in height (151 m considering its antenna), the Torre Pontina (Fig. 1) is the most imposing landmark in the Municipality of Latina and is one of the ten tallest buildings in Italy. The architectural design of the tower was conceived by architect Lodovico Risoli while the structural design was developed by engineers Massimo Guerrini and Luciano Gioacchini from SBG & Partners in Rome.

The tower consists of 37 floors above ground with a 3.10 m floor height, the layout of the floors is an octagon formed by a 34.60 m square shape from which an isosceles right triangle has been removed from each corner measuring 4.05 m (Fig. 2). The tower rests on a 40 x 40 m foundation plane and is supported by 136 piles that reach the depths of -40 m into the ground.

The vertical structure consists of 44 elements of various sizes (pillars and walls) in reinforced concrete, as reported in the plan in Fig. 2. The dimensions of these elements are shown in Table 1 and, for almost all elements, remain constant over the entire height of the building, forming a regular structure both in plan (double symmetry) and elevation.

A slight variation on the structure is present in the three highest floors of the building, where pillars P2, P5, P40 and P43 reduce their size from 3.7 m to 1 m. These variations will not be considered in this paper because they are considered to have little influence on the bending behaviour of the structure.

The horizontal structure consists of reinforced concrete slabs of 0.3 m of thickness, cast in situ and capable of connecting all the vertical structures. The load considered

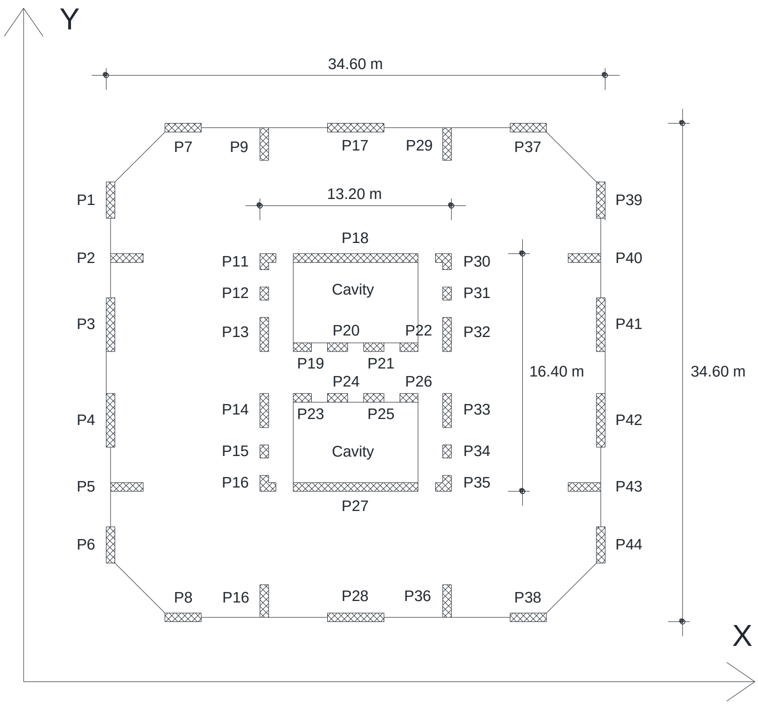

Fig. 2 Torre Pontina structural plan

Table 1 Dimensions of the Torre Pontina vertical structures

Pillar	X dimension [m]	Y dimension [m]
P1, P6, P39, P44	0.60	2.70
P2, P5, P40, P43	2.25	0.60
P3, P4, P41, P42	0.60	3.90
P7, P8, P37, P38	2.70	0.60
P9, P16, P29, P36	0.60	2.25
P11, P16, P30, P35	0.60 (thickness)	1.20 (exterior)
P12, P15, P31, P34	0.60	0.90
P13, P14, P32, P33	0.60	2.30
P17, P28	4.10	0.60
P18, P27	8.60	0.60
P19, P22, P23, P26	1.20	0.60
P20, P21, P24, P25	1.20	0.60

on the building is the wind load, evaluated in a static manner in accordance with Italian technical rules and regulations (NTC, 2008). For the sake of simplicity this study choses to consider a constant load along the height of the building equal to 63.6 kN/m (42.4 kN/m in pressure and 21.2 kN/m in depression) even though regulations propose a variable trend in the pressure along the building's height. The value of the constant load considered was determined on the basis of an average of the load values along the building's height and has the sole purpose of simplifying the mathematical process, without prejudice to the generality of the proposed approach. Since the structure is doubly symmetric and the load considered is a wind load in direction X (Fig. 2), the structural model is simplified by using a planar modelisation of the structural behaviour.

The following paragraph reports two solutions of reference that are adopted in order to compare the outcome achieved by the proposed approach with classical results based on consolidated theories and methods. Having comparative results, even if they are not guaranteed proof of the accuracy of the results obtained, is always useful in interpreting results and understanding the stronger and weaker points of a new approach.

3. Reference solutions evaluated through classical methods

In order to validate the proposed approach, two classical solutions have been developed: the first one is based on the solution of the Euler-Bernoulli elastic beam equation, while the second refers to the finite element method.

3.1 Solutions achieved with the classical Euler-Bernoulli equation

The Euler-Bernoulli differential beam equation (Eq. 1), solved (for a cantilever beam representing the building) by taking into consideration the relative boundary conditions (2), provides very approximate results.

$$E \cdot I \cdot \frac{dv^4(x)}{dx^4} = q(x) \tag{1}$$

$$\left. v(x) \right|_{x=0} = 0 \; ; \quad \left. \frac{dv(x)}{dx} \right|_{x=0} = 0 \; ; \quad \left. \frac{d^2v(x)}{dx^2} \right|_{x=L} = 0 \; ; \quad \left. \frac{d^3v(x)}{dx^3} \right|_{x=L} = 0 \tag{2}$$

In Eqs. (1)-(2), x is the beam abscissa that origins at the restrained end, $v(x)$ is the unknown transverse displacement function, $q(x)$ is the transverse load function, E is the Young's modulus, I is the value of the bending inertia of the section and L is the height of the building. In this context, the building is modelled as a vertical cantilever, fixed at its base and subjected to a constant horizontal load. The main source of the approximation lies in the impossibly of modelling the bending stiffness of the building properly. In fact, the building is modelled as a large vertical cantilever with only one section while the vertical structure is composed of many elements (pillars and walls) connected by deformable structural elements (slabs). The solutions of differential Eqs. (1)-(2) are given in Eqs. (3)-(4).

$$v(x) = \frac{q \cdot x^2}{24 \cdot E \cdot I} \cdot \left(x^2 - 4 \cdot L \cdot x + 6 \cdot L^2 \right) \tag{3}$$

$$\vartheta(x) = \frac{q \cdot x}{6 \cdot E \cdot I} \cdot \left(x^2 - 3 \cdot L \cdot x + 3 \cdot L^2 \right) \tag{4}$$

Due to the uncertainty regarding the value of I, Eqs. (3)-(4) will be used to evaluate two reference solutions. The first solution referred to as "EB – Min" (Euler-Bernoulli Minimum) uses only the inertia of the central core, neglecting the inertia of all the columns around the building. The value of this inertia, evaluated as if all elements of the central core were part of the section of a single element, was determined to be 558 m^4. The solution obtained with these data will approximate in excess the displacements of the structure. The second solution uses the inertia of all the vertical elements, considering them as part of a single section that remains flat and perpendicular to the neutral axis during the deformation process. In this case, the inertia is much greater (4687 m^4) and the solution in the displacements will be approximated by default. This second solution will be referred to as "EB – Max" (Euler-Bernoulli Maximum).

3.2 Solution achieved with a finite element method

In order to obtain a less approximated reference solution, a finite elements model was developed using the software ADINA (Bathe 1995). The building's structure was modelled using a planar model (Figs. 3 and 4) composed by three equivalent pillars and horizontal slabs. Two equivalent pillars are placed at the centres of gravity of the group of

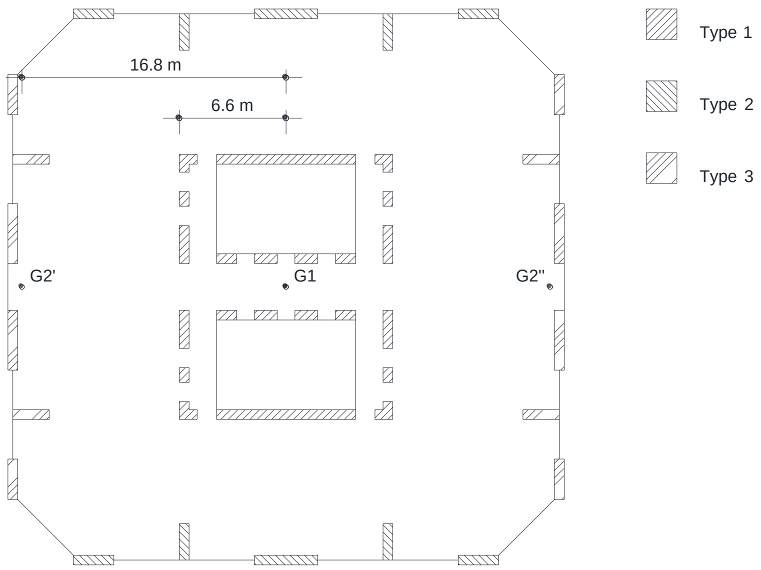

Fig. 3. Types of pillars considered in the numerical model

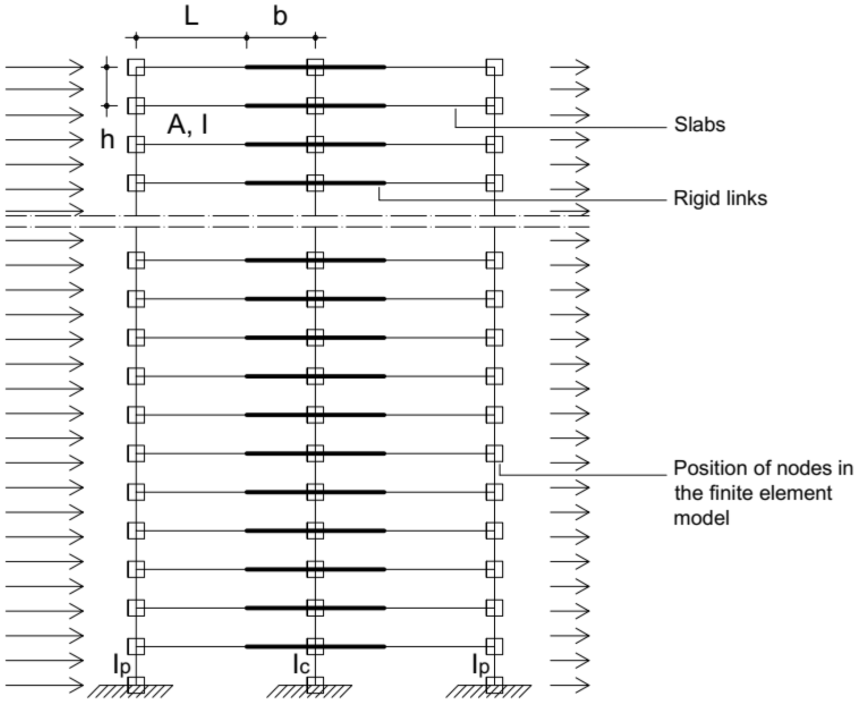

Fig. 4. Image of the finite elements model

pillars at the sides of the building (from P1 to P6 and from P39 to P44, type 1 elements in Fig. 3) and the third at the centres of gravity of the central core. For the first two equivalent pillars, area and inertia was assessed on the basis of the areas and inertias of the lateral pillars (P1 – P6 and P39 – P44) with reference to the centres of gravity G2' and G2'' (Fig. 3). The values of area and inertia of the equivalent pillars evaluated with this assumption are equal to $A = 10.62$ m^2, $I = 2.75$ m^4.

In the centre of gravity of the building (point G1 in Fig. 3) is placed an equivalent pillar to the central core of the building (type 2 elements in Fig. 3). Even for these elements, it is assumed that the structural behaviour is that of a single structural element. In this second case, this assumption is justified by the fact that, although between the various vertical elements there are openings (on average of 1.2 m) all the elements are connected by deep beams of 1.3 m of height. It is assumed that the presence of such beams is sufficient to restore a certain level of unity to the section. The area and inertia of the columns P7, P9, P17, P29, P 37 and P8, P16, P28, P36, P38 are added to the areas and inertias of the central element. The final value of the area and inertia of the central element are considered to equal 44.16 m^2 and 558 m^4 respectively.

For every floor, the reinforced concrete slab is modelled with beam elements with a base equal to the width of the

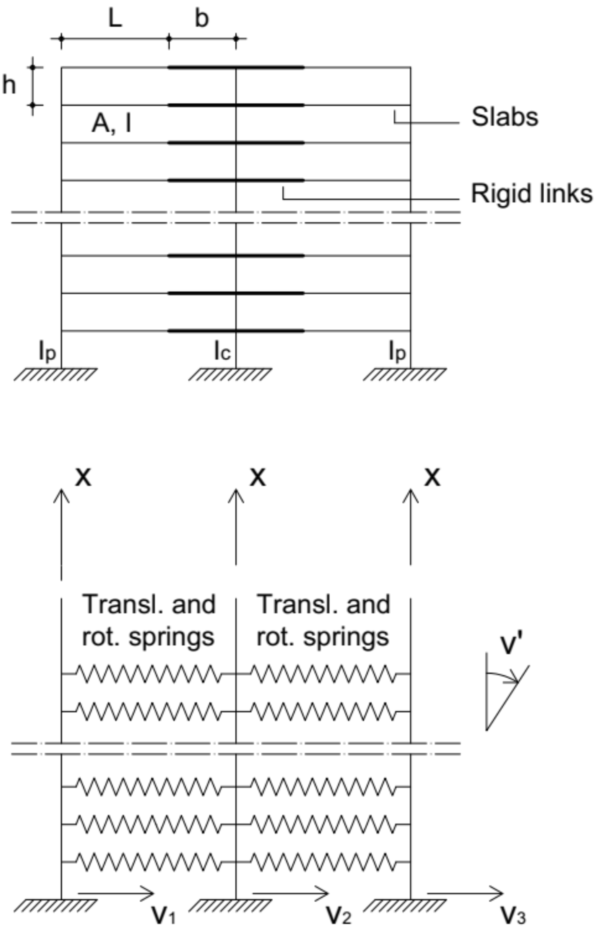

Fig. 5. Structural diagram and sign conventions assumed for the Multi-Beam approach

slab (34.6 m) and a thickness equal to the slab thickness (0.3 m). Since the central core has an important physical dimension (13.2 m), part of the elements representing the slabs are modelled as rigid elements in order to better approximate the stiffness of the floors. (6.6 m on every side of the central core as reported in Fig. 3). Fig. 4 shows the finite element model developed with the ADINA software.

4. Formulating of the multi-beam model

The Multi-Beam modelling approach to the structural problem is based on the simplifying hypothesis that the axial and flexural stiffness of the slabs can be distributed along the heights of the floors in a uniform manner. Such a hypothesis, very strong for modestly high buildings, seems more acceptable for high-rise buildings (if regular in elevation) made up of a significant number of floors. In relation to the diagrams in Fig. 5, the structural frame in the top part of the figure becomes composed of only a series of vertical beam elements interconnected by an infinite number of elastic springs.

In this manner it is possible to describe the flexural behaviour of the whole structure as a set of Euler-Bernoulli beams, one beam for every vertical element considered,

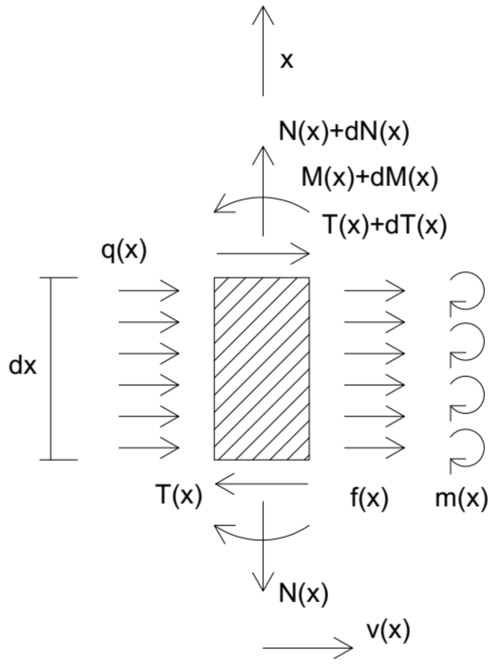

Fig. 6. Conventions assumed for writing equilibrium equations

coupled each other by the distributed stiffness of the floors. In (Sgambi and Sato 2019) the authors present the same approach of a high-rise buildings modelling but considering the axial stiffness of the slabs only.

The solution will be assessed numerically (finite differences) using the Matlab environment and will be compared with the results of the reference models (Section 3).

4.1 The equilibrium equations

By extracting an infinitesimal beam element from one of the three vertical elements in Fig. 5, the diagram in Fig. 6 can be obtained. In this diagram, in addition to the internal actions, *N(x)* (axial), *T(x)* (shear), *M(x)* (bending moment), the external transversal load *q(x)* it is shown together with the distributed force *f(x)* and the distributed momentum *m(x)* which the slabs transmit to the vertical structures.

Based on the conventions specified in Fig. 6, equilibrium can be carried out in a vertical direction and in rotation, leading to the Eq. (5):

$$\begin{cases} \dfrac{dT(x)}{dx} + q(x) + f(x) = 0 \\ \dfrac{dM(x)}{dx} - T(x) - m(x) = 0 \end{cases} \tag{5}$$

Differentiating the second equation and substituting the first inside the second, we get:

$$\frac{d^2M(x)}{dx^2} + q(x) + f(x) - \frac{dm(x)}{dx} = 0 \tag{6}$$

By introducing the relationship that links the bending moment to the curvature $\chi(x)$ and by assuming constant stiffness characteristics of the beam (E, I) along the height, we get the Eq. 7:

$$E \cdot I \cdot \frac{d^2\chi}{dx^2} + q(x) + f(x) - \frac{dm(x)}{dx} = 0 \tag{7}$$

Which becomes, with the sign conventions assumed for the mathematical curvature and the physical curvature ($\chi(x) = -dv^2(x)/dx^2$):

$$E \cdot I \cdot \frac{dv^4(x)}{dx^4} - f(x) + \frac{dm(x)}{dx} = q(x) \tag{8}$$

Eq. (8) is valid for every vertical structural element present in Fig. 5, then it is possible to write the following system of three equations:

$$\begin{cases} E \cdot I_1 \cdot \dfrac{dv_1^4(x)}{dx^4} - f_1(x) + \dfrac{dm_1(x)}{dx} = q_1(x) \\ E \cdot I_2 \cdot \dfrac{dv_2^4(x)}{dx^4} - f_2(x) + \dfrac{dm_2(x)}{dx} = q_2(x) \\ E \cdot I_3 \cdot \dfrac{dv_3^4(x)}{dx^4} - f_3(x) + \dfrac{dm_3(x)}{dx} = q_3(x) \end{cases} \tag{8}$$

where subscript 1 indicates that the Eq. 1 is relative to the equivalent pillar at the left, subscript 2 indicates the equation relative to the central core and subscript 3 indicates the equation relative to the equivalent right pillar. It is worth noting that the three equations are coupled with one another by the presence of the terms $f(x)$ and $m(x)$ which depend on the displacement functions $v_1(x)$, $v_2(x)$ and $v_3(x)$ and their derivatives. In the following section, these expressions will be made more explicit.

4.1 The axial contribution f(x)

Based on the transversal displacement functions $v_1(x)$, $v_2(x)$ and $v_3(x)$ and on the basis of the geometric and mechanical characteristics of the slab, when displacement occurs on the vertical elements, the slabs react with the following axial forces on the vertical elements:

$$\begin{cases} f_1(x) = \dfrac{E \cdot A}{L \cdot h} \cdot \left[v_2(x) - v_1(x) \right] \\ f_2(x) = \dfrac{E \cdot A}{L \cdot h} \cdot \left[-v_2(x) + v_1(x) + v_3(x) - v_2(x) \right] \\ f_3(x) = -\dfrac{E \cdot A}{L \cdot h} \cdot \left[v_3(x) - v_2(x) \right] \end{cases} \tag{9}$$

where E is the Young's modulus of the slab, A is its area and L the length of its deformable part (Fig. 5). h is the floor-to-floor height and its presence in the denominator of (9) allows to consider the axial forces originating from the floors as uniformly distributed on the vertical elements. By assigning the term k_a to the fraction outside the brackets in Eq. 9, we can rewrite Eq. 9 in the following system:

$$\begin{cases} f_1(x) = k_a \cdot \left[v_2(x) - v_1(x) \right] \\ f_2(x) = k_a \cdot \left[v_1(x) - 2 \cdot v_2(x) + v_3(x) \right] \\ f_3(x) = -k_a \cdot \left[v_3(x) - v_2(x) \right] \end{cases} \tag{10}$$

4.3 The flexural contribution m(x)

The flexural contribution is assessed in the same way in which the axial contribution was analysed. Based on the sign conventions adopted (Fig. 5), three rotations are imposed on the vertical elements: $v'_1(x)$, $v'_2(x)$ e $v'_3(x)$. By using the beam's elastic coefficients (the coefficients of the displacement method), the bending moments caused by slabs deformation on the vertical elements are evaluated. A slight algebraic complication is caused by the presence of the rigid link of length b (Fig. 5) needed to model the physical presence of the central core. Superposing all contributions, the Eq. 11 is obtained.

$$\begin{cases} m_1(x) = \dfrac{1}{h} \cdot \left(\dfrac{4 \cdot E \cdot I}{L} \right) \cdot \dfrac{dv_1(x)}{dx} \\ + \dfrac{1}{h} \cdot \left(\dfrac{2 \cdot E \cdot I}{L} + \dfrac{6 \cdot E \cdot I}{L^2} \cdot b \right) \cdot \dfrac{dv_2(x)}{dx} \\ m_2(x) = \dfrac{1}{h} \cdot \left(\dfrac{2 \cdot E \cdot I}{L} + \dfrac{6 \cdot E \cdot I}{L^2} \cdot b \right) \cdot \dfrac{dv_1(x)}{dx} \\ + \dfrac{1}{h} \cdot \left(\dfrac{8 \cdot E \cdot I}{L} + \dfrac{24 \cdot E \cdot I}{L^2} \cdot b + \dfrac{24 \cdot E \cdot I}{L^3} \cdot b^2 \right) \cdot \dfrac{dv_2(x)}{dx} + \\ + \dfrac{1}{h} \cdot \left(\dfrac{2 \cdot E \cdot I}{L} + \dfrac{6 \cdot E \cdot I}{L^2} \cdot b \right) \cdot \dfrac{dv_3(x)}{dx} \\ m_3(x) = \dfrac{1}{h} \cdot \left(\dfrac{2 \cdot E \cdot I}{L} + \dfrac{6 \cdot E \cdot I}{L^2} \cdot b \right) \cdot \dfrac{dv_2(x)}{dx} \\ + \dfrac{1}{h} \cdot \left(\dfrac{4 \cdot E \cdot I}{L} \right) \cdot \dfrac{dv_3(x)}{dx} \end{cases} \tag{11}$$

Where I is the inertia of the horizontal structure, L is its deformable length and b is the length of rigid links (Fig. 5). Also, in this case, the presence of the height of the floors h in the denominator of Eq. (11) is needed to redistribute the bending stiffness of the slabs on the height of the floors. Eq. (11) can be rewritten in a more compact form:

$$\begin{cases} m_1(x) = k_{f1} \cdot \dfrac{dv_1(x)}{dx} + k_{f2} \dfrac{dv_2(x)}{dx} \\ m_2(x) = k_{f2} \cdot \dfrac{dv_1(x)}{dx} + k_{f3} \cdot \dfrac{dv_2(x)}{dx} + k_{f2} \cdot \dfrac{dv_3(x)}{dx} \\ m_3(x) = k_{f2} \cdot \dfrac{dv_2(x)}{dx} + k_{f1} \cdot \dfrac{dv_3(x)}{dx} \end{cases} \tag{12}$$

Where the following relations are posed:

$$k_{f1} = \frac{1}{h} \cdot \left(\frac{4 \cdot E \cdot I}{L} \right) \tag{13}$$

$$k_{f2} = \frac{1}{h} \cdot \left(\frac{2 \cdot E \cdot I}{L} + \frac{6 \cdot E \cdot I}{L^2} \cdot b \right) \tag{14}$$

$$k_{f3} = \frac{1}{h} \cdot \left(\frac{8 \cdot E \cdot I}{L} + \frac{24 \cdot E \cdot I}{L^2} \cdot b + \frac{24 \cdot E \cdot I}{L^3} \cdot b^2 \right) \tag{15}$$

4.4 The solving system

By inserting Eqs. (10) and (12) into Eq. (8), it is possible to get a system of three ordinary differential equations which models the behaviour of the building used as a case study.

$$\begin{cases} E \cdot I_1 \cdot \dfrac{dv_1^4(x)}{dx^4} - k_{f1} \cdot \dfrac{d^2 v_1(x)}{dx^2} \\ -k_{f2} \cdot \dfrac{d^2 v_2(x)}{dx^2} - k_a \cdot \left[v_2(x) - v_1(x) \right] = q_1(x) \\ E \cdot I_2 \cdot \dfrac{dv_2^4(x)}{dx^4} - k_{f2} \cdot \dfrac{d^2 v_1(x)}{dx^2} - k_{f3} \cdot \dfrac{d^2 v_2(x)}{dx^2} - k_{f2} \cdot \dfrac{d^2 v_3(x)}{dx^2} + \\ \quad - k_a \cdot \left[v_1(x) - 2 \cdot v_2(x) + v_3(x) \right] = q_2(x) \\ E \cdot I_3 \cdot \dfrac{dv_3^4(x)}{dx^4} - k_{f2} \cdot \dfrac{d^2 v_2(x)}{dx^2} \\ -k_{f1} \cdot \dfrac{d^2 v_3(x)}{dx^2} + k_a \cdot \left[v_3(x) - v_2(x) \right] = q_3(x) \end{cases} \tag{16}$$

Eq. (16) must be solved under the correct boundary conditions. For this case study, for every vertical element, the following conditions must be imposed:

$$v(x)\Big|_{x=0} = 0 \; ; \quad \left. \frac{dv(x)}{dx} \right|_{x=0} = 0 \; ; \quad M(x)\Big|_{x=L} = 0 \; ; \quad T(x)\Big|_{x=L} = 0 \tag{17}$$

which represent the fixed end conditions at the base and free end at the top. It is worth noting that, if the bending moment condition (Eq. 18) is transformed into the classical condition that imposes a null value for the second derivative of the displacement, the shear condition, due to the presence of distributed momentum *m(x)*, becomes:

$$T_i(x)\Big|_{x=L} = E \cdot I_i \cdot \frac{d^3 v_i(x)}{dx^3} - m_i(x) \Bigg|_{x=L} = 0 \tag{18}$$

where the expressions of $m_i(x)$ are reported in Eq. (12) and depends on which vertical element is considered.

4.5 Internal actions assessment

The displacement functions derive directly from the solution of the system of ordinary differential equations as presented in Eq. (16) and (17). The internal actions in the vertical elements can be found on the basis of the considerations regarding equilibrium and kinematic relationships. For the bending moment, it can be found with the classical equation:

$$M_i(x) = E \cdot I_i \cdot \frac{d^2 v_i(x)}{dx^2} \tag{19}$$

In order to assess the shear action, we need to consider not only the third derivative of the displacement, but also the distributed bending moment load, originating from the slabs:

$$T_i(x) = E \cdot I_i \cdot \frac{d^3 v_i(x)}{dx^3} - m_i(x) \tag{20}$$

The axial actions in the vertical elements can be assessed on the basis of equilibrium considerations. The vertical elements have to collect the shear actions from the slabs. Using elastic coefficients of the beam, we can arrive at the distributed axial action on the vertical elements:

$$\begin{aligned} n_1(x) &= \frac{6 \cdot E \cdot I}{L^2} \cdot \frac{1}{h} \cdot v_1'(x) \\ &+ \left(\frac{6 \cdot E \cdot I}{L^2 \cdot h} + \frac{12 \cdot E \cdot I}{L^3} \cdot \frac{b}{h} \right) \cdot v_2'(x) \end{aligned} \tag{21}$$

$$n_1(x) = -\frac{6 \cdot E \cdot I}{L^2} \cdot \frac{1}{h} \cdot v_1'(x) + \frac{6 \cdot E \cdot I}{L^2} \cdot \frac{1}{h} \cdot v_3'(x) \tag{22}$$

$$\begin{aligned} n_1(x) &= -\left(\frac{6 \cdot E \cdot I}{L^2} \cdot \frac{1}{h} + \frac{12 \cdot E \cdot I}{L^3} \cdot \frac{b}{h} \right) \cdot v_2'(x) \\ &- \frac{6 \cdot E \cdot I}{L^2} \cdot \frac{1}{h} \cdot v_3'(x) \end{aligned} \tag{23}$$

and hence assess the axial action in the elements through an integration:

$$N_i(x) = \int_{H-x}^{H} n_i(x) \cdot dx \tag{24}$$

The system of ordinary differential equations (Eq. 16) is solved within its boundary conditions (Eq. 17) numerically using the Matlab environment. The next paragraph will discuss the results obtained from the reference formulations and the proposed formulation. For the last formulation, the acronym MB (Multi-Beam formulation) will be used.

5. Discussion of the results

Fig. 7 illustrates the results in terms of displacement function $v_2(x)$, representing the flexion in a vertical plane of the central core. It is worth noting how, in general, the horizontal displacement is very small (the maximum displacement under wind load reaches only a few centimetres).

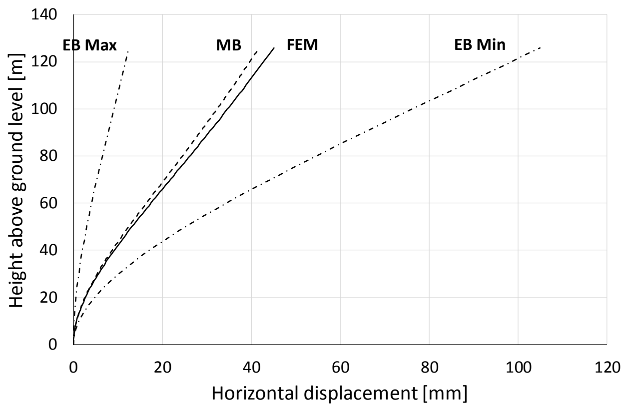

Fig. 7. Horizontal displacement curves of the central core assessed with the Euler-Bernoulli equation (EB Max with I assessed considering all vertical elements, EB Min with I assessed considering only the inertia of the central core), with a planar finite element model (FEM) and with the proposed Multi-Beam approach (MB)

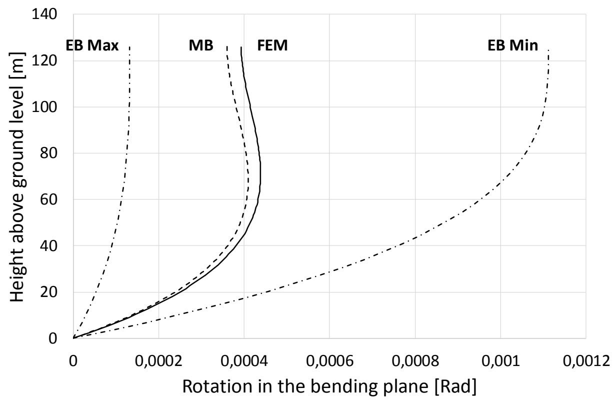

Fig. 8. Rotation curves along the flexion plane of the central core assessed with the Euler-Bernoulli equation (EB Max with I assessed considering all vertical elements, EB Min with I assessed considering only the inertia of the central core), with a planar finite element model (FEM) and the proposed Multi-Beam approach (MB)

This result is due to the presence, in the building, of a very strong vertical structure (walls with 60 cm of thickness and a central core measuring approximately 13 m) which remains constant throughout the building's height. In relation to the solutions evaluated with a finite elements model, the solution to the Euler-Bernoulli equation is significantly different, both in its EB - Max formulation and in its EB – Min formulation. The solution to the proposed system of equations (Eq. 16) leads to a maximum error of 5% compared to the finite elements solution, which appears slightly more flexible. It must be noted that the finite elements model is able to consider the axial deformability of the vertical elements, while in the proposed formulation, these elements was assumed to be rigid in axial direction.

Fig. 8 shows the diagram of the central core's rotation $v_2'(x)$ in the vertical flexion plane. Once again, it is worth noting how the two curves assessed with the two solutions of reference EB – Max and EB – Min are significantly distant from the curve assessed by finite elements modelling and how the solution that can be obtained from the proposed formulation (MB) is very close to the finite elements model's solution (FEM). The graphs also show that the shape of the EB curves is significantly different from the shape of the FEM and MB curves. In these last two curves the angle of rotation decreases in the value of in the upper part of the building.

As regards internal actions, Fig. 9 reproduces the shear action on the central core. The EB curve is obtained using the Euler-Bernoulli theory and gives us a maximum shear action value at the base of 8000 kN which decreases linearly to zero, proceeding towards the top of the building. It is worth noting that the EB solution does not differentiate between the shear action on the central core and the shear action on the lateral pillars, the value 8000 kN is simply equal to the resultant of the horizontal load taken into consideration. The FEM solution, on the other hand, presents a "steps" solution with a constant value of shear action across the floors and jumps corresponding to the slabs' locations, where the horizontal load is transmitted to

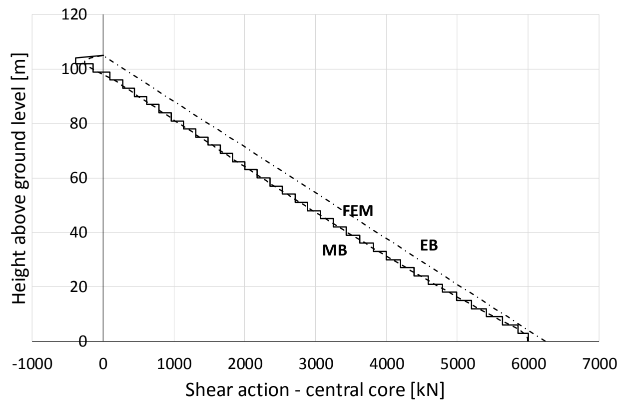

Fig. 9 Curves representing the shear action on the central core assessed with the Euler-Bernoulli equation (EB), with a planar finite element model (FEM) and with the proposed Multi-Beam approach (MB)

the central core. Also worthy of note is that the maximum shear action value is slightly lower than in the EB solution since in the FEM solution a small portion of shear action is on the lateral columns.

The MB model result is based on the solution of Eqs. (16), (17) and (20).This solution is not able to describe the punctual jumps in shear action at the slab level; however it can provide an average description of the values. Worthy of note (Fig. 9) is how this solution is in perfect agreement with the FEM model solution. Again, in the MB solution the maximum shear action on the central core (7705 kN) is lower than the resultant of the horizontal load since also in this formulation a small portion of load is taken from the lateral pillars.

The bending moment diagrams on the central core (Fig. 10) show a classic parabolic shape for the EB solution. The FEM model produces a significantly lower bending moment maximum value (298 MNm compared to 503 MNm for the EB solution). Such a difference is due to the presence of the lateral columns which are capable of balancing a portion of the overturning momentum caused from the wind load by a

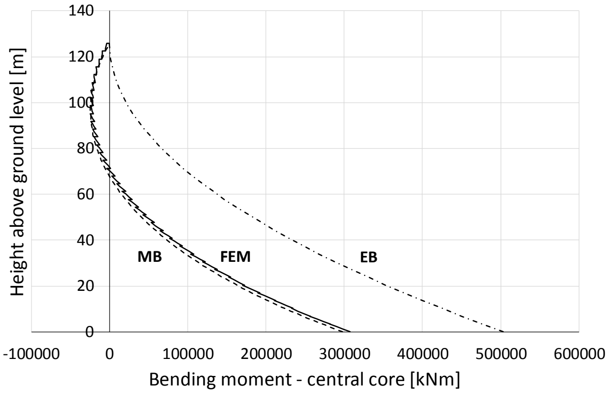

Fig. 10. Curves representing the Bending Moment on the central core assessed via the Euler-Bernoulli equation (EB), with a planar finite element model (FEM) and with the proposed Multi-Beam approach (MB)

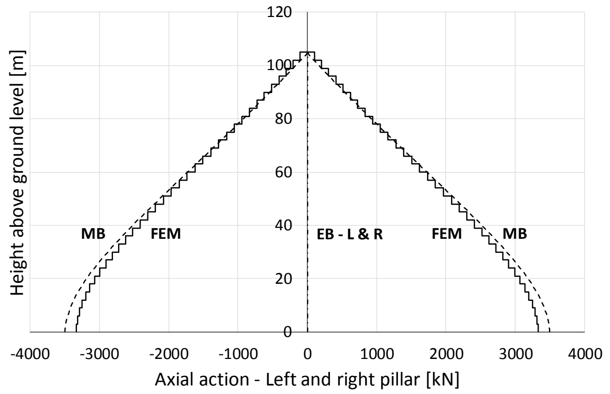

Fig. 11. Curves representing the Axial Action on the lateral columns assessed via the Euler-Bernoulli equation (EB), with a flat finite element model (FEM) and with the proposed Multi-Beam approach (MB)

rocking effect. The EB model is not able to reproduce this resistant mechanism therefore the total value of the overturning momentum must to be supported in terms of bending moment on central core. The proposed MB model is able to capture this aspect. In fact, the horizontal structures (beams and slabs) are the ones that couple together the flexural behaviour of the central core with the axial mechanism of the external pillars. The proposed MB model provides, once more, a solution that is significantly close to that of the FEM model.

Fig. 11 underlines this rocking resistant mechanism with a graph showing the axial actions in the external pillars. The EB solution leads to a null value for the axial action while the FEM model and the MB model lead to two curves that are very close to one another. It is worth noting that by multiplying the maximum value of the MB model’s axial action (or that of the FEM model) by the distance between the two equivalent lateral columns, it is possible to get: 5930 x 33,6 = 199 MNm which is the difference between the maximum moment at the base as evaluated with the EB model and that evaluated with the MB (or FEM) model.

Table 2 shows the error calculated with regards to the reference solution for the finite elements of the two

Table 2 Error % assessed in relation to the finite element reference solution

	EB - Max	MB	EB - Min
Horizontal displacement	72.3	7.32	133
Rotation in the bending plane	66.4	8.40	182
Shear action (central core)	3.81	0.0130	3.81
Bending moment (central core)	63.3	3.25	63.3
Axial action (lateral pillar)	100	4.77	100

differential formulations considered. The error is calculated at the top of the building for horizontal displacement and rotation and at the base of the internal actions.

As described in the introduction, the approach proposed in this paper is less effective and less efficient than the approaches proposed by Cuni *et al.* (2013) and Fujita *et al.* (2015) but does not require any parameters calibration procedure.

From the point of view of the efficiency, once the problem was formulated analytically, in this paper the solution was assessed numerically. The number of unknown variables needed to obtain the solution is greater than the one required for the Cuni *et al.* (2013) and Fujita *et al.* (2015) models but less than the one required for a similar finite element model (Section 3.2).

From the point of view of the accuracy, the proposed model does not take into account the shear deformability of structural elements, since it was developed on the basis of Eulero Bernoulli's classical theory. On this point, we can notice that the importance of shear deformability in an MB model is less important than in Cuni *et al.* (2013) and Fujita *et al.* (2015) models, where the building is modelled as a single cantilever element.

In the proposed approach, the vertical elements (central core and pillars) are in fact modelled as separate elements. The behaviour of the central core is flexural and involves the entire height of the building (the ratio length/deep of the element is about 10). For the lateral columns, the contribution of shear deformability is more important. However, the proposed MB modelling is not able to capture the shear deformability between two floors because the horizontal elements appear distributed on the vertical elements. Such imprecision is intrinsic to this type of modelling. Probably, by using a different theory to develop the MB model and through an identification process (as in the models of Cuni *et al.* 2013 and Fujita *et al.* 2015) it would be possible to improve this aspect.

6. Conclusion

This paper provides a novel approach for modelling high-rise buildings subjected to a static horizontal load. The approach presented is an approach based on the formulation of a set of fourth-degree differential equations equal to the number of vertical structures (columns or walls) contained in the building (ODE). This formulation is presented in reference to an existing 37-floor building, modelled as a planar frame. Thus, only three vertical structures are taken into consideration for the model, which reproduce, in an equivalent way, the stiffness of the outer columns of the building and central core. By distributing the stiffness of the slabs along the height of the floors, we get a structural model composed of three Euler-Bernoulli beams interconnected by an infinite amount of springs. This model (MB), which can operate with a variable number of Euler-Bernoulli beams, is a generalisation of the double-beam systems which are already studied by the literature. The formulation, applied to the selected case study, leads to a system of three ordinary fourth-degree differential equations, which must be solved using the necessary boundary conditions.

The same building was modelled using the finite elements method, assuming the same modelling hypotheses (FEM).

By comparing the results, it becomes clear that the proposed model is capable of reproducing the results that are obtainable with a similar finite elements model with an error of around 5% and is also capable of describing mechanisms that a simplified cantilever model is not able to reproduce (for example, the resistant mechanism provided by the axial action in the exterior columns).

If the proposed approach is compared with other approaches in the literature (Cuni *et al*. 2013, Fujita *et al*. 2016), it can be seen that the proposed MB modelling is a more approximate approach because it does not take into account the shear deformability of the elements. However, the approach has two advantages. A first advantage over the two approaches mentioned is that no calibration procedure is required. The proposed approach can be directly used for any high-rise building with the same characteristics of the studied building and for any type of load. A second advantage of the proposed modelling is that the formulation is analytical. This can lead to a symbolic solution of the equations that govern the problem.

Further developments of the approach may also concern the possibility to model the 3D behaviour of the building or the introduction of a dynamic load.

Dedication

In memory of Noemi Basso, a friend and esteemed colleague of Waseda University who recently passed away. A flower too delicate to overcome the storms of life.

References

Abu-Hilal, M. (2006), "Dynamic response of a double Euler–Bernoulli beam due to a moving constant load", *J. Sound Vib.*, **297**, 477–491. https://doi.org/10.1016/j.jsv.2006.03.050.

Akgoz, B. and Civalek, O. (2011), "Nonlinear vibration analysis of laminated plates resting on nonlinear two-parameters elastic foundations", *Steel Compos. Struct.*, **11**, 403–421. https://doi.org/10.12989/scs.2011.11.5.403.

Alavi, A. and Rahgozar, R. (2018), "Optimal stiffness distribution in preliminary design of tubed-system tall buildings", *Struct. Eng. Mech.*, **65**(6), 731-739. https://doi.org/10.12989/sem.2018.65.6.731.

Asai, T. and Watanabe, Y. (2017), "Outrigger tuned inertial mass electromagnetic transducers for high-rise buildings subject to long period earthquakes", *Eng. Struct.*, **153**, 404-410. https://doi.org/10.1016/j.engstruct.2017.10.040.

Aydin, S. and Bozdogan, K.B. (2016), "Lateral stability analysis of multistory buildings using the differential transform method", *Struct. Eng. Mech.*, **57**(5), 861-876. https://doi.org/10.12989/sem.2016.57.5.861.

Avini, R., Kumar, P., Hughes, S.J. (2019), "Wind loading on high-rise buildings and the comfort effects on the occupants", *Sustainable Cities Soc.*, **45**, 378-394. https://doi.org/10.1016/j.scs.2018.10.026.

Barbato, M., Palmeri, A. and Petrini, F. (2014), "Special Issue on Performance-based engineering, Editorial foreword", *Eng. Struct.*, **78**, 1-2. http://dx.doi.org/10.1016/j.engstruct.2014.10.001.

Barretta, R., Canadija, M. and Marotti de Sciarra, F. (2015), "A higher-order Eringen model for Bernoulli–Euler nanobeams", *Arch. Appl. Mech.*, **86**, 483-495, https://doi.org/10.1007/s00419-015-1037-0.

Bateson, G. (1979), *Mind and Nature: A Necessary Unity*, New Ed. (31 January 2002), Hampton Press, New York, USA.

Bathe, K.J. (1995), *Finite Element Procedures*, MIT, Pearson College Education Inc., USA.

Bathe, K.J. (2019), "The AMORE paradigm for finite element analysis", *Adv. Eng. Software*, **130**, 1-3. https://doi.org/10.1016/j.advengsoft.2018.11.010.

Bayat, M. and Pakar, I. (2015), "Mathematical solution for nonlinear vibration equations using variational approach", *Smart Struct. Syst.*, **15**(5), 1311-1327. https://doi.org/10.12989/sss.2015.15.5.1311.

Bayat, M. and Pakar, I. (2017), "Analytical study on non-natural vibration equations", *Steel Compos. Struct.*, **24**(6), 671-677. https://doi.org/10.12989/scs.2017.24.6.671.

Brunesi, E., Nascimbene, R., Casagrande L. (2016), "Seismic analysis of high-rise mega-braced frame-core buildings", *Eng. Struct.*, **115**, 1-17. http://dx.doi.org/10.1016/j.engstruct.2016.02.019.

Civalek, O. and Acar, M.H. Discrete singular convolution method for the analysis of Mindlin plates on elastic foundations. *J. Pressure Vessels Piping*, **84**(9), 527–535. https://doi.org/10.1016/j.ijpvp.2007.07.001.

Civalek, O. and Kiracıoglu, O. (2010), "Free vibration analysis of Timoshenko beams by DSC method", *J. Numerical Methods Biomedical Eng.*, **26**, 1890-1898. https://doi.org/10.1002/cnm.1279.

Cyrus, N.J. and Fulton, R.E. (1966), "Finite Difference Accuracy in Structural Analysis", *J. Struct. Division*, **92**(6), 459-471.

Falsone G. (2018), "The use of generalized functions modeling the concentrated loads on Timoshenko beams", *Struct. Eng. Mech.*, **67**(4), 385-390. https://doi.org/10.12989/sem.2018.67.4.385.

Feras, H., Darwish, F.H., Al-Nimr, M.A. and Hatamleh, M.I. (2015), "Thermoelastic analysis for a slab made of a thermal diode-like material", *Struct. Eng. Mech.*, **53**(4), 645-659. https://doi.org/10.12989/sem.2015.53.4.645.

Franchin, P., Petrini, F., Mollaioli, F. (2018), "Improved risk-targeted performance-based seismic design of reinforced concrete frame structures", *Earthq. Eng. Struct. Dynam.*, **47**(1), 49-67. https://doi.org/10.1002/eqe.2936.

Fujita, K., Ikeda, A., Shirono, M. and Takewaki, I. (2015), "System identification of high-rise buildings using shear-bending model and ARX model: Experimental investigation", *Earthq. Struct.*, **8**(4), https://doi.org/10.12989/eas.2015.8.4.843.

Garavaglia, E., Pizzigoni, A., Sgambi, L. and Basso N. (2013), "Collapse behaviour in reciprocal space frame structures", *Struct. Eng. Mech.*, **46**(4), 533-547. https://doi.org/10.12989/sem.2013.46.4.533.

Han, F., Dan, D. and Cheng, W. (2018), "An exact solution for dynamic analysis of a complex double-beam system", *Compos. Struct.,* **193**, 295-305. https://doi.org/10.1016/j.compstruct.2018.03.088.

Lazzari, P.M., Filho, A.C., Lazzari, B.M., Pacheco, A.R. and Gomes, R.R.S. (2019), "Numerical simulation of the constructive steps of a cable-stayed bridge using ANSYS", *Struct. Eng. Mech.*, **69**(3), 269-281. https://doi.org/10.12989/sem.2019.69.3.269.

Lee, D., Ha, T., Jung, M. and Kim, J. (2014), "Evaluating high performance steel tube-framed diagrid for high-rise buildings", *Steel Compos. Struct.*, **16**(3), 289-303, https://doi.org/10.12989/scs.2014.16.3.289.

Liu, S. and Yang, B. (2019), "A closed-form analytical solution method for vibration analysis of elastically connected double-beam systems", *Compos. Struct.*, **212**, 598-608. https://doi.org/10.1016/j.compstruct.2019.01.038.

Lou, G.B. and Wang, A.J. (2015), "Studies into a high performance composite connection for high-rise buildings", *Steel Compos. Struct.*, **19**(4), https://doi.org/10.12989/scs.2015.19.4.789.

Malerba, P.G. and Sgambi, L. (2014), "Riveted steel elements deformed by the swelling of interstitial rust. A study on a residual bearing capacity", *Proceedings of the 7th International Conference on Bridge Maintenance, Safety and Management* (IABMAS 2014), Shanghai, China, 7-11 July 2014.

Manju, S. and Mukherjee, S. (2019), "Function space formulation of the 3-noded distorted Timoshenko metric beam element", *Struct. Eng. Mech.*, **69**(6), 615-626. https://doi.org/10.12989/sem.2019.69.6.615.

Niiranen, J. and Niemi, A.H. (2017), "Variational formulations and general boundary conditions for sixth-order boundary value problems of gradient-elastic Kirchhoff plates", *Europ. J. Mech. A/Solids*, **61**, 164-179. https://doi.org/10.1016/j.euromechsol.2016.09.001.

NTC2018 (2018), "Norme tecniche per le costruzioni - D.M. 17 Gennaio 2018", *Supplemento ordinario alla Gazzetta Ufficiale n. 42, del 20 febbraio 2018 - Serie generale*, Rome, Italy.

Oniszczuk, Z. (2000), "Free transverse vibrations of elastically connected simply supported double-beams complex system", *J. Sound Vib.*, **232**, 387-403. https://doi.org/10.1006/jsvi.1999.2744.

Pavlović, R., Kozić, P. and Pavlović, I. (2012), "Dynamic stability and instability of a double-beam system subjected to random forces", *J. Mech. Sci.*, **62**(1), 111-119. https://doi.org/10.1016/j.ijmecsci.2012.06.004.

Petrini, F., Giaralis, A. and Wang, Z. (2020), "Optimal tuned mass-damper-inerter (TMDI) design in wind-excited tall buildings for occupants' comfort serviceability performance and energy harvesting", *Eng. Struct.*, **204**, 109904, https://doi.org/10.1016/j.engstruct.2019.109904.

Qiao, S., Han, X., Zhou, K. and Li, W. (2017), "Conceptual configuration and seismic performance of high-rise steel braced frame", *Steel Compos. Struct.*, **23**(2), 229-251. https://doi.org/10.12989/scs.2017.23.2.173.

Tien, P.W. and Calautit, J.K. (2019), "Numerical analysis of the wind and thermal comfort in courtyards "skycourts" in high rise buildings", *J. Build. Eng.*, **24**, article 100735. https://doi.org/10.1016/j.jobe.2019.100735.

Timoshenko, S. (1970), *Theory of Elasticity*, McGraw-Hill College; 3 edition, New York, USA.

Samanipour, K. and Vafai, H. (2015), "Congestion effect on maximum dynamic stresses of bridges", *Struct. Eng. Mech.*, **55**(1), 111-135. https://doi.org/10.12989/sem.2015.55.1.111.

Park, H.S., Lee, E., Choi, S.W., Oh, B.K., Cho, T. and Kim. Y. (2016), "Genetic-algorithm-based minimum weight design of an outrigger system for high-rise buildings", *Eng. Struct.*, **117**, 496-505. https://doi.org/10.1016/j.engstruct.2016.02.027.

Shahrzad Soudian, S. and Berardi, U. (2017), "Experimental investigation of latent thermal energy storage in high-rise residential buildings in Toronto", *Energy Procedia*, **132**, 249-254. https://doi.org/10.1016/j.egypro.2017.09.706.

Sofi M., Lumantarna E., Zhong A., Mendis P.A. and Barnes R. (2018), "Determining dynamic characteristics of high rise buildings using interferometric radar system", *Eng. Struct.*, **164**, 230-242. https://doi.org/10.1016/j.engstruct.2018.02.084.

Sgambi, L., Basso, N., Pavani, R., Civelli, E., Meroni, C.D. and Pagin, M. (2013), "Numerical models of a beam belonging to a tall building: errors and approximations within ordinary design", *Proceedings of the 2nd International Conference on Structures and Architecture*, Guimaraes, Portugal, 24-26 July 2013.

Sgambi, L., Garavaglia, E., Basso, N. and Bontempi, F. (2014), "Monte Carlo simulation for seismic analysis of a long span suspension bridge". *Eng. Struct.*, **78**, 100-111. https://doi.org/10.1016/j.engstruct.2014.08.051.

Sgambi, L. (2016), "Modélisation des structures: une science (in)exacte", *LieuxDits*, **14**, 9-15.

Sgambi, L. and Sato, B. (2019), "High-rise building modelling: numerical and analytical approaches", *Proceedings of the 4nd International Conference on Structures and Architecture*, Guimaraes, Portugal, 24-26, July.

Vu, H.V., Ordonez, A.M. and Karnopp, B.H. (2000), "Vibration of a double-beam system", *J. Sound Vib.*, **229**, 807-822. https://doi.org/10.1006/jsvi.1999.2528.

Wallerstein, D.W. (2001), *A Variational Approach to Structural Analysis*, Wiley-Interscience, New Jersey, USA.

Wang, T.F., Lu, N.L. and Lan, P. (2016), "Analytical method for the out-of-plane buckling of the jib system with middle strut", *Steel Compos. Struct.*, **21**(5), 963-980. https://doi.org/10.12989/scs.2016.21.5.963.

Wu, X., Li, Y. and Zhang, Y. (2017), "Elasto-plastic time history analysis of a 117-story high structure", *Comput. Concrete*, **19**(1), 7-17. https://doi.org/10.12989/cac.2017.19.1.007.

PL